ISET Journal of Earthquake Technology, Paper No. 544, Vol. 56, No. 3, September 2019, pp. 57-74

RANDOM RESPONSE ANALYSIS OF PARALLEL STRUCTURES CONNECTED WITH MAXWELL DAMPER

C.C. Patel

Department of Civil Engineering
Marwadi Education Foundation Group of Institution
Rajkot - 360003, India
E-mail: *ccstruct@gmail.com*

ABSTRACT

In this paper, the response behavior of two parallel single-degree-of-freedom structures connected with Maxwell damper is studied under base acceleration modeled as a non-stationary random process as well as stationary white-noise random excitation. The governing equations of motion of the connected structures are formulated and root mean square responses (relative displacement and absolute acceleration) are obtained. The responses are obtained considering 1000 ground motion realization using Monte Carlo simulation. The influence of parameters such as relaxation time of damper, frequency, and mass ratio of structures on the performance of damper is investigated. For undamped coupled structures, the closed-form expressions for optimum damper damping for the minimum value of mean square relative displacement and absolute acceleration of either of coupled structures are derived.

KEYWORDS: Maxwell Damper, Parallel Structures, Seismic Effect

INTRODUCTION

Earthquake ground motions transmit additional energy input to structures and sometimes structure becomes more susceptible to inelastic deformation. The inelastic deformation leads to non-structural as well as structural damage and sometimes catastrophic failure. The conventional design approach of designing a structure with adequate ductility to absorb excess energy during natural disturbances, sufficient strength to withstand natural forces and appropriate stiffness to maintain structural integrity and serviceability, allows inelastic cyclic deformations in specially detailed regions of a structure. It provides the minimum level of protection to the structures and may render a structure irreparable. The seismic protection of structures is a challenging task for the civil engineering community. The use of energy dissipation devices and control mechanisms into the structure is another approach for seismic protection of structures. These control strategies can dynamically the response of the structure in a desirable manner, thereby termed protective systems for the new structures. Moreover, existing structures can be retrofitted or strengthened effectively by structural control to withstand future seismic activity. Housner et al. [1] presented the tutorial/survey paper on Structural Control: Past, Present, and Future. They have discussed the passive control, active control, semi-active control, hybrid control, sensors for structural control, smart material systems and health monitoring and damage detection. Soong and Spencer [2] presented the state-of-the-art and state-of-the-practice on supplemental energy dissipation devices. They also describe the advantages and limitations of supplemental energy dissipation devices in the context of seismic design and retrofit of civil engineering structures. Dutta [3] presented a state-of-the-art review on active control of structures. The review includes the theoretical backgrounds of different active control schemes, limitations, and difficulties of their practical implementation and a brief introduction on semi-active control. The above review and some other studies confirm the efficacy of seismic protection of the structure using energy dissipation devices. Commonly used passive energy dissipation devices are friction dampers, viscous dampers, viscoelastic dampers, metallic yielding dampers, lead extrusion damper, tuned mass, or tuned liquid dampers. Full-scale damper tests and analysis in 5 story steel frame Kasai et al. [4], the current status of passive control of buildings in Japan Kasai et al. [5] and other past study confirm that the passive control devices are found to be effective for seismic response control of structures [6]. The excellent treatises by Soong and Dargush [7] and Constantinou et al. [8] give more complete details on the mechanics and working principles of these devices. The fluid viscoelastic device operates on the principle of resistance of viscous fluid flow through specially shaped orifices. To simplify the mathematical analysis, the force deformation relationship of fluid orifice damper is often modeled by the linear viscous model, in which the damper force is directly proportional to the relative velocity of damper ends. Such model gives rise to damping forces that are out-of-phase with deformation and deformation dependent forces. At higher frequencies of deformation, the damper force of majority orifice dampers would be displacement dependent and thus provide stiffness to the system. Different mathematical models have been proposed which capture this frequency-dependent stiffening behavior of fluid orifice damper. The experimental investigation by Constantinou and Symans [9] on seismic response of buildings with supplemental fluid dampers shows that the fluid damper exhibits viscoelastic fluid behavior. To account for this viscoelastic behavior, the simplest model is the Maxwell model in which the force-deformation relationship is described by a first-order differential equation. The frequency-dependent characteristic is introduced by the spring element in series with the viscous dashpot. Makris and Constantinou [10] proposed the Maxwell model for seismic isolation of building structures and validated it by dynamic testing. Singh et al. [11] presented the optimal distribution and the parameters of the Maxwell damper in a structure subjected to seismic excitation using a gradient-based optimization scheme. Lewandowski and Chorazyczewski [12] presented the methods for the identification of the parameters of the Maxwell fractional model and Kelvin-Voigt fraction model. Greco and Marano [13] presented the parameter identification for basic and generalized Kelvin-Voigt and Maxwell models for fluid viscous dampers using particle swarm optimization. The parameters of the generalized Maxwell model from the fraction Zener model have been determined based on the equivalence of complex modulus in the frequency domain and presented a detailed comparison of the performance of generalized Maxwell model and fractional Zener model [14].

Interactions between existing neighboring inadequately separated buildings are frequently recurrent problems during the strong earthquake. Due to different dynamic properties, adjacent structures can vibrate out of phase during earthquake excitations and creates relative displacement problems. The various problems are like, a collapse can occur when the common vertical support share by structures and the distance between supporting structures increases, for example falling off bridge deck from supports. When the distance between vibrating structures decreases, pounding of the structures may occur, a more dangerous condition during an earthquake [15]. The restrainer provided to limit the separation distance between adjacent structures are subjected to severe puling which may result in local failure and/or undesirable inertia forces transfers from one segment to the other one of the bridge [16]. Amongst various structural control techniques, connecting parallel structures by passive energy dissipation devices (when possible) is an effective alternative for seismic response mitigation. The concept is to exert control force upon one another to reduce the overall response of the dynamically dissimilar coupled structures. But it alters the dynamic characteristics of the unconnected structures. It enhances undesirable torsional response when the structures have asymmetric geometry and increase the base shear of the stiff structure. In certain situations, the free space available between parallel structures can be effectively utilized for the installation of control devices.

Zhang and Xu [17] studied the random seismic response of adjacent buildings linked by dampers using the state-space method and pseudo-excitation method. The effectiveness of the fluid damper and beneficial damper relaxation time and damping coefficient at zero frequency have been investigated. An experimental seismic study of adjacent buildings with fluid dampers was carried out by Yang et al. [18]. The fluid damper control force was considered the linear force-velocity property. The results showed that the fluid damper of proper parameters could significantly reduce the seismic response of connected buildings while the natural frequencies of both buildings remained almost unchanged. It was also observed that to achieve good control performance, the number, location, and linking pattern of fluid dampers should be properly selected. Zhu and Xu [19] presented the analytical formulae for the response of adjacent single-degree-of-freedom (SDOF) structures connected by the Maxwell model. The optimum damper parameters have been derived using the principle of minimizing the averaged vibration energy of the coupled system. Matsagar and Jangid [20] presented the seismic response analysis of base- isolated adjacent buildings connected with visco-elastic dampers. The analysis results show that for the existing under-designed fixed base structure, the base isolation of both or one of the adjacent building found advantageous in the retrofitting works. Bhasakararao and Jangid [21] have studied the dynamic behavior of two adjacent SDOF structures connected with a viscous damper. The close-form expressions are derived for optimum damper damping and corresponding steady-state mean square displacement and absolute acceleration response of either of the connected structure. Patel and Jangid [22] investigated the performance of Maxwell dampers connecting two adjacent multi-degree-of-freedom (MDOF) structures under real earthquake excitations. Zhu et al. [23] presented the optimized parameter of connecting dampers between two adjacent structures. The optimization criteria are minimizing the vibration energy of both the structure as well as minimizing the vibration energy of the primary structure. Milanchian et al. [24] investigated the performance of viscous and viscoelastic link interconnecting the vertically isolated structures. An earthquake phenomenon is random in nature, so probabilistic analysis of the energy dissipation device connected parallel structures system subjected to random process gives more appropriate results. In this paper, the response behavior of parallel SDOF structures connected by Maxwell model-defined fluid damper subjected to a non-stationary random process is investigated. The analytical expression for harmonic transfer function for displacement and absolute acceleration response of either of the connected structure is presented. The response of the coupled structure subjected to non-stationary as well as a stationary random process is analyzed. The effect of various system parameters on the performance of damper is evaluated. The close-form expression for optimum damper damping and the corresponding mean square responses under stationary white noise random excitation is obtained.

PARALLEL STRUCTURES CONNECTED BY MAXWELL DAMPER

Let us consider two parallel SDOF structures connected with the Maxwell model defined fluid damper as shown in Figure 1, referred to as Structure 1 and 2, respectively. The coupled structures are symmetric with their symmetric planes in the alignment. The ground motion is to occur in the direction of the symmetric planes of the structures. The ground acceleration under both structures is assumed to be the same. The considered parallel structures is modeled as a linear SDOF system and due to the significant increase of energy absorbing capacity the structures can retain elastic and linear properties under the ground motion excitation. The effect of soil-structure interaction is neglected. Let m_1, k_1, c_1 and m_2, k_2, c_2 be the mass, stiffness and damping coefficient of the Structure 1 and 2, respectively. Let $\omega_1 = \sqrt{k_1/m_1}$ and $\omega_2 = \sqrt{k_2/m_2}$ be the circular frequencies and $\xi_1 = c_1/2m_1\omega_1$ and $\xi_2 = c_2/2m_2\omega_2$ be the damping ratios of Structures 1 and 2, respectively. Let us consider two parameters mass ratio (μ) and frequency ratio (β) of the connected structures defined as

$$\mu = \frac{m_1}{m_2} \tag{1}$$

$$\beta = \frac{\omega_2}{\omega_1} \tag{2}$$

The damper force f_d can be described by the first order Maxwell model proposed by Bird et al. [25] given as

$$f_d + \lambda \frac{df_d}{dt} = c_d(\dot{x}_r) \tag{3}$$

λ is the relaxation time defined by

$$\lambda = c_d / k_d \tag{4}$$

where c_d is the damper damping coefficient at zero frequency, k_d is the damper stiffness coefficient and $\dot{x}_r$ is the relative velocity of damper ends. The non-dimensional damping ratio at zero frequency (ξ_d) and relaxation time (χ) are defined as

$$\xi_d = \frac{c_d}{2m_1\omega_1} \tag{5}$$

$$\chi = \lambda\omega_1 \tag{6}$$

The governing equations of motion for the damper-connected system can be written as

$$m_1\ddot{x}_1 + c_1\dot{x}_1 + k_1x_1 + f_d = -m_1\ddot{x}_g \tag{7}$$

$$m_2\ddot{x}_2 + c_2\dot{x}_2 + k_2x_2 - f_d = -m_2\ddot{x}_g \tag{8}$$

where x_1 and x_2 are displacement response relative to the ground of Structure 1 and 2, respectively; over dot represent time derivative; and $\ddot{x}_g$ is the ground acceleration. The damper is connecting two parallel structures at their floor level; hence the relative velocity of damper ends is given as $\dot{x}_r = \dot{x}_1 - \dot{x}_2$. The structural control criteria depend on the nature of dynamic loads and the response quantities of interest. In case of stiff structure, acceleration is of more concern generating higher inertia force in the structure, should be mitigated, whereas, in case of flexible structure displacement is predominant that needs to be controlled. Thus, minimizing relative displacement and/or absolute acceleration of the system has always been considered as the control objective. In view of this, the study aims to evaluate the performance of Maxwell damper for minimizing exclusively displacement as well as acceleration responses of coupled structure.

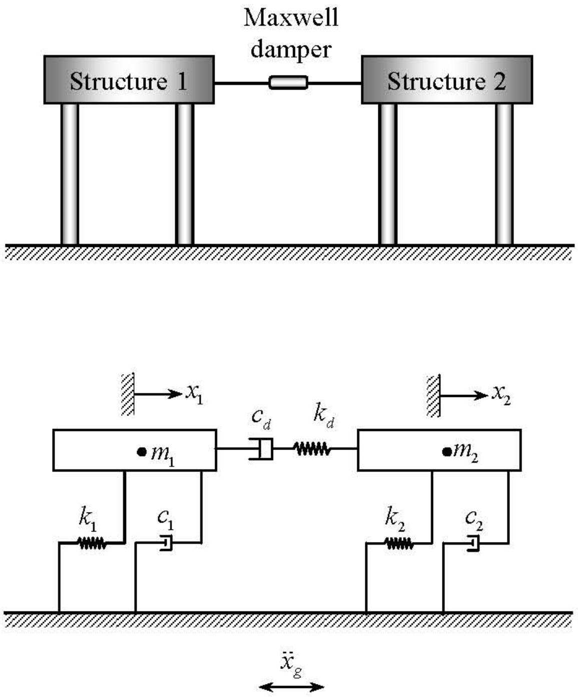

Fig. 1 Structural model of two SDOF parallel structures connected with Maxwell damper and its corresponding mathematical model

GROUND MOTION EXCITATION

Earthquake ground motions are multidimensional and random in nature. Various kinds of stochastic ground motion models, stationary or non-stationary have been developed, which describe the uncertainties characterizing earthquake ground motion time histories. Housner [26], Thomson [27], Rosenblueth and Bustamante [28] and many others, earlier proposed stationary white noise earthquake models. The stationary filtered white noise models suggested by Kanai [29] and Tajimi [30] describe the dominant frequency and local site properties in the ground motion. It was used extensively in random vibration analysis of structures. The stationary models fail to reproduce amplitude non-stationary (time-varying intensity) typical of real earthquake ground motion time histories. Therefore, different kinds of time-modulating functions were introduced to produce various non-stationary ground motion models. If the evolution of the frequency content with time can be neglected, the amplitude non-stationary of ground-motion is modeled by a stationary Gaussian random process with zero mean multiplied by a deterministic modulating function also called envelop function. The modulating function capture the non-stationary trend observed in earthquake ground motion excitation. The various envelop function generally used are exponential type envelop function by Shinozuka and Sato [31], Iyenger and Iyenger [32], Box-car type modulating function by Tajimi [30], initially increasing parabolic, remain constant during strong motion duration, and decaying exponentially suggested by Amin and Ang [33] and many others. The earthquake excitation $\ddot{x}_g(t)$ is expressed as

$$\ddot{x}_g(t) = A(t)\,\ddot{x}_f(t) \tag{9}$$

where $A(t)$ is a deterministic modulating function; and $\ddot{x}_f(t)$ is a stationary random process. The evolutionary power spectral density function (PSDF) of the earthquake excitation is given by

$$S_{\ddot{x}_g}(\omega) = |A(t)|^2\, S_{\ddot{x}_f}(\omega) \tag{10}$$

where $S_{\ddot{x}_f}(\omega)$ is stationary PSDF of the earthquake ground motion. In the present study, the PSDF of the earthquake excitation $\ddot{x}_f(t)$ is considered as (Clough and Penzien) [34]

$$S_{\ddot{x}_f}(\omega) = S_0 \left(\frac{1 + 4\xi_s^2 (\omega/\omega_s)^2}{\left[1 - (\omega/\omega_s)^2\right]^2 + 4\xi_s^2 (\omega/\omega_s)^2} \right) \left(\frac{(\omega/\omega_f)^4}{\left[1 - (\omega/\omega_f)^2\right]^2 + 4\xi_s^2 (\omega/\omega_f)^2} \right) \tag{11}$$

where S_0 is constant PSDF of input white-noise random process; and ω_s, ξ_s, ω_f and ξ_f are ground filter parameters. The ω_s and ξ_s generally represent the predominant frequency and damping ratio of soil strata, respectively. To model the various shape of the PSDF of earthquake excitation, the different values of the parameters ω_f and ω_s is to be considered. The random process $\ddot{x}_f(t)$ is considered as the response of two linear filters subjected to white-noise excitation as

$$\ddot{x}_f(t) + 2\xi_f\omega_f\dot{x}_f(t) + \omega_f^2 x_f(t) = -\left(\ddot{x}_s(t) + \ddot{x}_0(t)\right) \tag{12}$$

$$\ddot{x}_s(t) + 2\xi_s\omega_f\dot{x}_s(t) + \omega_s^2 x_s(t) = -\ddot{x}_0(t) \tag{13}$$

where $\ddot{x}_0(t)$ is input white-noise random process with the constant intensity of the PSDF S_0. The Equations (12) and (13) provide the stationary PSDF of the response $\ddot{x}_f(t)$ as that expressed by Equation (11). The non-stationary response of SDOF system for different shapes of modulating function having the same energy content has been presented by Jangid [35]. In the present study the non-stationary earthquake excitation $\ddot{x}_g(t)$ is the non-stationary random process $\ddot{x}_f(t)$ to be obtained considering the input white-noise random process $\ddot{x}_0(t)$, and modulating function $A(t)$, proposed by Amin and Ang [33]. The modulating function initially increases parabolic (up to time t_1), remain constant during strong motion (between t_1 and t_2), and then decreases exponentially, expressed as

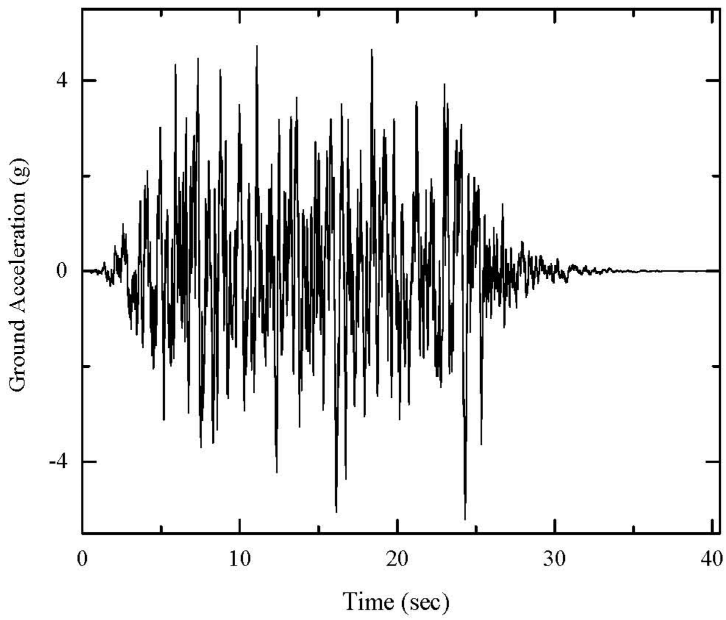

Fig. 2 Typical non-stationary ground motion realization

$$A(t) = \begin{cases} (t/t_1)^2 & (0 \le t \le t_1) \\ 1 & (t_1 \le t \le t_2) \\ e^{-c(t-t_2)} & (t \ge t_2) \end{cases} \tag{14}$$

where c is constant. A typical non-stationary ground motion realization with parameters t_1 = 5 sec, t_2 = 20 sec, strong motion duration t_2 - t_1 = 15 sec, and $c = 0.5$ s^{-1} is shown in Figure 2.

NUMERICAL STUDY

Two parallel SDOF structures with identical mass (i.e. mass ratio μ = 1) connected at floor level by Maxwell damper is considered. The lateral stiffness of each structure is chosen in such a way that the fundamental circular frequency of Structure 1 is π rad/sec and that of Structure 2 is 2π rad/sec. Thus, Structure 1 may be considered as a flexible structure and Structure 2 as a stiff structure. The frequency ratio β of the coupled structure becomes 2, (i.e. dynamically well-separated structures). The various parameters considered are the damping ratio of both the structure $\xi_1 = \xi_2 = 0.05$, the damping ratio of Maxwell damper $\xi_d = 0.21$ and relaxation time χ = 0.01. Considering 1000 realization of the input process and using ensemble averages, the root mean square (RMS) responses are obtained using extensive Monte Carlo simulation which is based on the equations of motion (Equations 3, 7, 8, 9, 12 and 13) of the coupled structure. For the present study, the various parameter $\omega_f = \pi/2$ rad/s, $\omega_s = 3\pi$ rad/s, $\xi_s = 0.6$, $\xi_f = 0.6$ and $S_0 = 0.05$ m^2/s^3 are used. The time variation of RMS relative displacement and RMS absolute acceleration of Structure 1 and 2 for non-stationary ground excitation (Clough and Penzien model) with damper and without damper is shown in Figure 3. It is observed that the stationary response is achieved in a short time and remains stationary during strong motion duration. The RMS response of parallel structures is decreased when they are connected with Maxwell damper. Similar behavior also observed in Figure 4, which shows the time variation of RMS relative displacement and RMS absolute acceleration of coupled structure subjected to stationary ground motion excitation. Considering the average value of RMS response during the strong motion duration phase as a response quantity, the percentage reduction in response quantities of the coupled structure is shown in Table 1. The variation of the RMS displacement response and RMS acceleration response against the damping ratio ξ_d is shown in Figure 5. It is observed that RMS response reduces up to the certain value of ξ_d after which they are increased. Thus there is some optimum value of ξ_d for which RMS response quantity is a minimum value. The optimum ξ_d value for displacement as well as the acceleration response of both the structure is different. But, at the optimum ξ_d value of any one response quantity, the other responses also decrease. The optimum value of ξ_d for one response quantity is close to the optimum value ξ_d of the other response quantity and in the vicinage of it, the response of the structures does not vary significantly. From Table 1 it is observed that the percentage reduction in the response quantities under non-stationary earthquake ground motion is quite comparable with that of the stationary response. The response of the considered structure to such non-stationary excitation involves lengthy calculation and much time-consuming. The other study also found that the response of structures to non-stationary excitations, both in the time domain (Gasparini [36], Langley [37], Muscolino [38] and many others) and frequency domain (Hammond [39], Corots and Vanmarcke [40] and many others) is complicated and involves lengthy calculations. Thus, to simplify the analysis, all subsequent numerical results are presented considering the Maxwell damper connected parallel structures subjected to white-noise earthquake excitation.

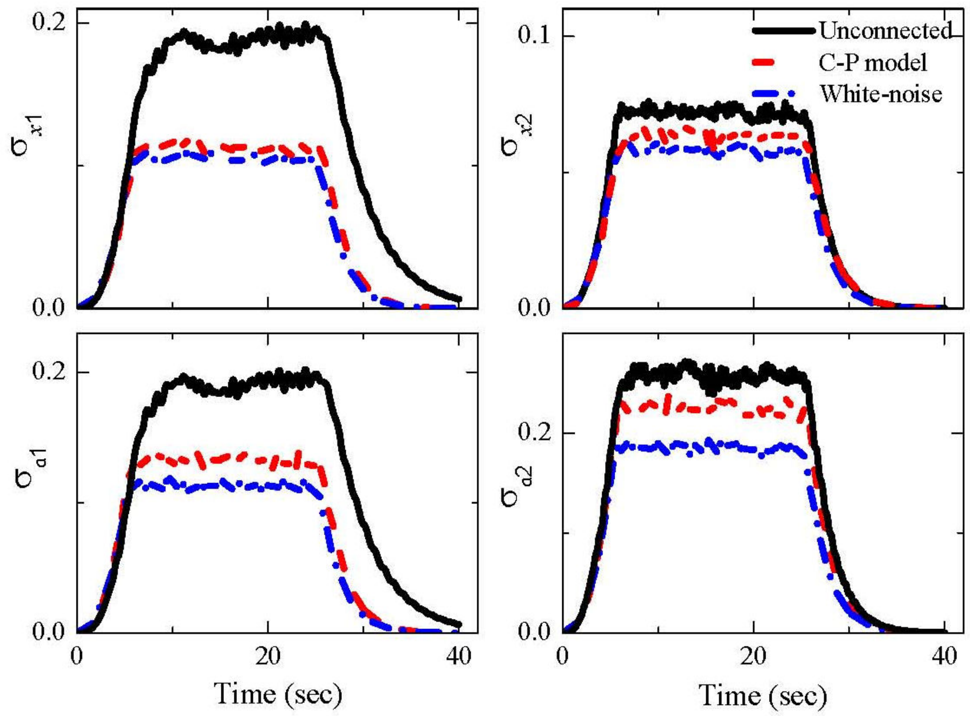

Fig. 3 Time variation of root mean square displacement and root mean square acceleration for non-stationary ground excitation

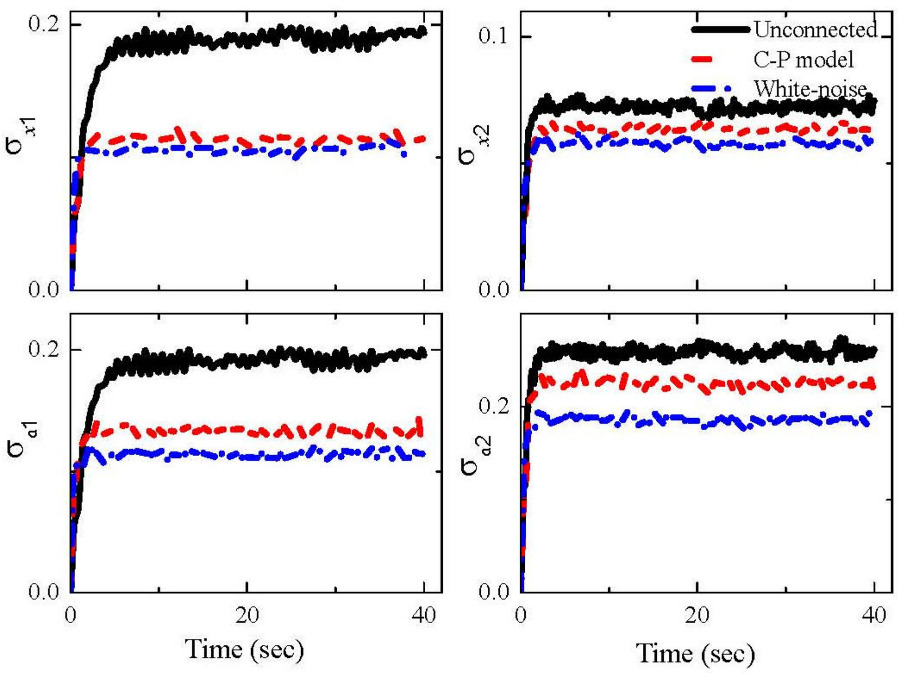

Fig. 4 Time variation of root mean square displacement and mean square acceleration for stationary excitation

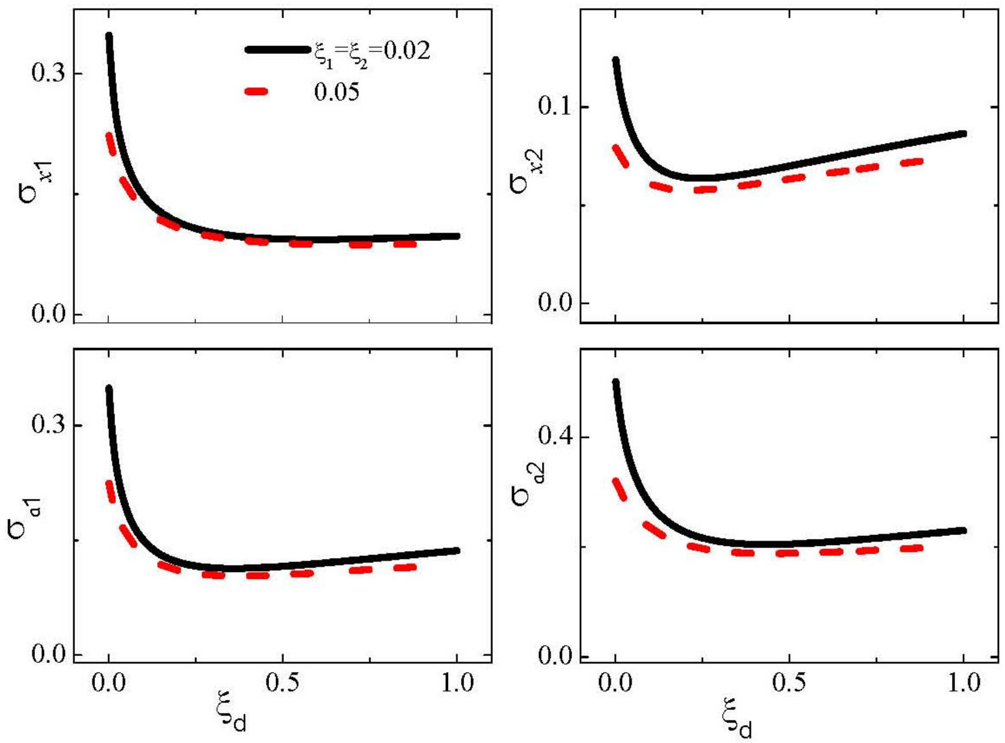

Fig. 5 Variation of root mean square responses against the damping coefficient of the damper for different value of structural damping in parallel structure ($\beta=2,\ \mu=1$ and $\chi=0.01$)

Table 1: Comparison of stationary and non-stationary responses of parallel structures connected by Maxwell damper (μ = 1, β = 2, $\xi_1=\xi_2=0.05$, χ = 0.01, ξ_d = 0.21 & S_0 = 0.05 m²/s³)

Model of PSDF of earthquake excitation	Response quantity	Stationary response	Non-stationary response
Clough and Penzien model with $\omega_f=\pi/2$ rad/s and $\omega_s=3\pi$ rad/s	RMS displacement x_1 (mm)	0.1885	0.1886
		0.1135 (39.79)*	0.1129 (40.14)
	RMS displacement x_2 (mm)	0.072	0.0718
		0.0637 (11.53)	0.0634 (11.70)
	RMS acceleration $\ddot{x}_{a1}$ (g)	0.1916	0.1914
		0.1327 (30.74)	0.1324 (30.83)
	RMS acceleration $\ddot{x}_{a2}$ (g)	0.2588	0.2579
		0.2241 (13.41)	0.2234 (13.38)
White-noise model	RMS displacement x_1 (mm)	0.1781	0.1709
		0.1060 (40.48)	0.1060 (37.98)
	RMS displacement x_2 (mm)	0.0575	0.0575
		0.0531 (7.65)	0.05254 (8.70)
	RMS acceleration $\ddot{x}_{a1}$ (g)	0.1807	0.1766
		0.1133 (37.30)	0.1133 (35.84)
	RMS acceleration $\ddot{x}_{a2}$ (g)	0.2160	0.2138
		0.1853 (14.21)	0.1853 (13.33)
*indicates percentage reduction in response for damper connected structure			

RESPONSE TO STATIONARY WHITE-NOISE RANDOM EXCITATION

The parallel structures connected with Maxwell damper subjected to stationary white-noise excitation, the mean square displacement response (σ_{x1}^2 and σ_{x2}^2) and acceleration response (σ_{a1}^2 and σ_{a2}^2) of Structure 1 and 2, respectively, are given by Nigam [41].

$$\sigma_{x1}^2 = \int_{-\infty}^{\infty} \left|x_1(\omega)\right|^2 S_0 d\omega \tag{15a}$$

$$\sigma_{x2}^2 = \int_{-\infty}^{\infty} \left|x_2(\omega)\right|^2 S_0 d\omega \tag{15b}$$

$$\sigma_{a1}^2 = \int_{-\infty}^{\infty} \left|\ddot{x}_{a1}(\omega)\right|^2 S_0 d\omega \tag{15c}$$

$$\sigma_{a2}^2 = \int_{-\infty}^{\infty} \left|\ddot{x}_{a2}(\omega)\right|^2 S_0 d\omega \tag{15d}$$

where $\left|x_1(\omega)\right|$ and $\left|x_2(\omega)\right|$ are the harmonic transfer function of displacement response of Structure 1 and 2, respectively; $\left|\ddot{x}_{a1}(\omega)\right|$ and $\left|\ddot{x}_{a2}(\omega)\right|$ are the harmonic transfer function for acceleration response of Structure 1 and 2, respectively. To obtain the harmonic transfer function for displacement and acceleration response, let us consider the connected structure as shown in Figure 1, is subjected to harmonic base acceleration given by

$$\ddot{x}_g = a_0 e^{i\omega t} \tag{16}$$

where a_0 and ω are the amplitude and excitation frequency, respectively, of the harmonic ground motion. This analysis is carried out in the frequency domain. Thus, from Equations 7, 8 and 16 the steady-state displacement response of Structure 1 and 2, is obtained as

$$x_1 = \frac{N_1}{D} a_0 e^{i\omega t} \text{ and } x_2 = \frac{N_2}{D} a_0 e^{i\omega t} \tag{17a, b}$$

where

$$N_1 = (i\omega)^4 \lambda^2 + (i\omega)^3 (\lambda^2 \Delta_2) + (i\omega)^2 (-1 + \lambda((1+\mu)\Delta_d + \lambda\omega_2^2)) + (i\omega)(-\Delta_2 - (1+\mu)\Delta_d) - \omega_2^2 \tag{18a}$$

$$N_2 = (i\omega)^4 \lambda^2 + (i\omega)^3 (\lambda^2 \Delta_1) + (i\omega)^2 (-1 + \lambda((1+\mu)\Delta_d + \lambda\omega_1^2)) + (i\omega)(-\Delta_1 - (1+\mu)\Delta_d) - \omega_1^2 \tag{18b}$$

$$\begin{aligned} D = {} & (i\omega)^6(-\lambda^2) + (i\omega)^5(-\lambda^2(\Delta_1+\Delta_2)) + (i\omega)^4(1 - \lambda^2\Delta_1\Delta_2 - \lambda((1+\mu)\Delta_d + \lambda(\omega_1^2+\omega_2^2))) \\ & + (i\omega)^3((1+\mu)\Delta_d - \Delta_2(-1+\lambda(\Delta_d+\lambda\omega_1^2)) - \Delta_1(-1+\lambda\mu\Delta_d+\lambda^2\omega_2^2)) \\ & + (i\omega)^2(\Delta_2\Delta_d + \Delta_1(\Delta_2+\mu\Delta_d) + (1-\lambda\mu\Delta_d)\omega_1^2 + (1-\lambda(\Delta_d+\lambda\omega_1^2))\omega_2^2) \\ & + (i\omega)((\Delta_2+\mu\Delta_d)\omega_1^2 + (\Delta_1+\Delta_d)\omega_2^2) \\ & + \omega_1^2\omega_2^2 \end{aligned} \tag{18c}$$

with $\Delta_1 = c_1/m_1$; $\Delta_2 = c_2/m_2$ and $\Delta_d = c_d/m_1$

The absolute acceleration response ($\ddot{x}_{a1}$ and $\ddot{x}_{a2}$) can be calculated by differentiating Equations (17) twice and adding it to the ground acceleration [Equation (16)] as given below

$$\ddot{x}_{a1} = \left(\ddot{x}_1 + \ddot{x}_g\right) = \frac{N_{a1}}{D} a_0 e^{i\omega t} \text{ and } \ddot{x}_{a2} = \left(\ddot{x}_2 + \ddot{x}_g\right) = \frac{N_{a2}}{D} a_0 e^{i\omega t} \tag{19}$$

where

$$\begin{aligned}N_{a1} &= (i\omega)^5(-\lambda^2\Delta_1)+(i\omega)^4\lambda^2(\Delta_1\Delta_2-\omega_1^2)+(i\omega)^3(-\lambda\Delta_2(\Delta_d+\lambda\omega_1^2)+\Delta_1(1-\lambda\mu\Delta_d-\lambda^2\omega_2^2))\\ &+(i\omega)^2(\Delta_2\Delta_d+\Delta_1(\Delta_2+\mu\Delta_d)+(1-\lambda\mu\Delta_d)\omega_1^2-\lambda(\Delta_d+\lambda\omega_1^2)\omega_2^2)\\ &+(i\omega)((\Delta_2+\mu\Delta_d)\omega_1^2+(\Delta_1+\Delta_d)\omega_2^2)+\omega_2^2\omega_1^2\end{aligned} \tag{20a}$$

$$\begin{aligned}N_{a2} &= (i\omega)^5(-\lambda^2\Delta_2)+(i\omega)^4\lambda^2(\Delta_1\Delta_2-\omega_2^2)+(i\omega)^3(-\lambda\Delta_1(\mu\Delta_d+\lambda\omega_2^2)+\Delta_2(1-\lambda(\Delta_d+\lambda\omega_1^2))\\ &+(i\omega)^2(\mu\Delta_1\Delta_d+\Delta_2(\Delta_1+\Delta_d)-\lambda\mu\Delta_d\omega_1^2+(1-\lambda(\Delta_d+\lambda\omega_1^2))\omega_2^2)\\ &+(i\omega)((\Delta_2+\mu\Delta_d)\omega_1^2+(\Delta_1+\Delta_d)\omega_2^2)+\omega_2^2\omega_1^2\end{aligned} \tag{20b}$$

The variation of the displacement response amplitude and acceleration response amplitude of two structures against the damping coefficient of the damper ξ_d, considering other parameters mass ratio μ = 1, frequency ratio β = 2 and relaxation time χ = 0.01 is shown in Figure 6 for different damping ratios in connected structures (i.e. $\xi_1=\xi_2=0$, 0.02, 0.05). It is observed that there exists an optimum value of the damping coefficient of the damper for minimum responses. It is also observed that the optimum damper damping coefficient for connected damped structures lies almost very close to that of connected undamped structures and a slight variation in the optimum damping of damper does not have much effect on the optimum responses. The difference in resulting responses of the damped system considering (a) actual optimum damper damping and (b) optimum damper damping that corresponding to the undamped system is quite negligible. Thus, the optimum damping coefficient for an undamped structure can also be used for the connected damped structure satisfactorily. To study the effect of relaxation time on the response of connected structural, the variation of responses against the excitation frequency considering mass ratio μ = 1, frequency ratio β = 2; structural damping $\xi_1=\xi_2=0.05$ and damping coefficient of damper ξ_d = 0.23 for different value of relaxation time (i.e. χ = 0.001, 0.01, 0.1, 1, 10) is shown in Figure 7. It is observed that the displacement, as well as acceleration response of Structure 1, is not affected by the relaxation time (χ) value less than 0.1, whereas, for Structure 2, the effect of the relaxation time (χ) value less than 0.01 not affecting the displacement and acceleration response.

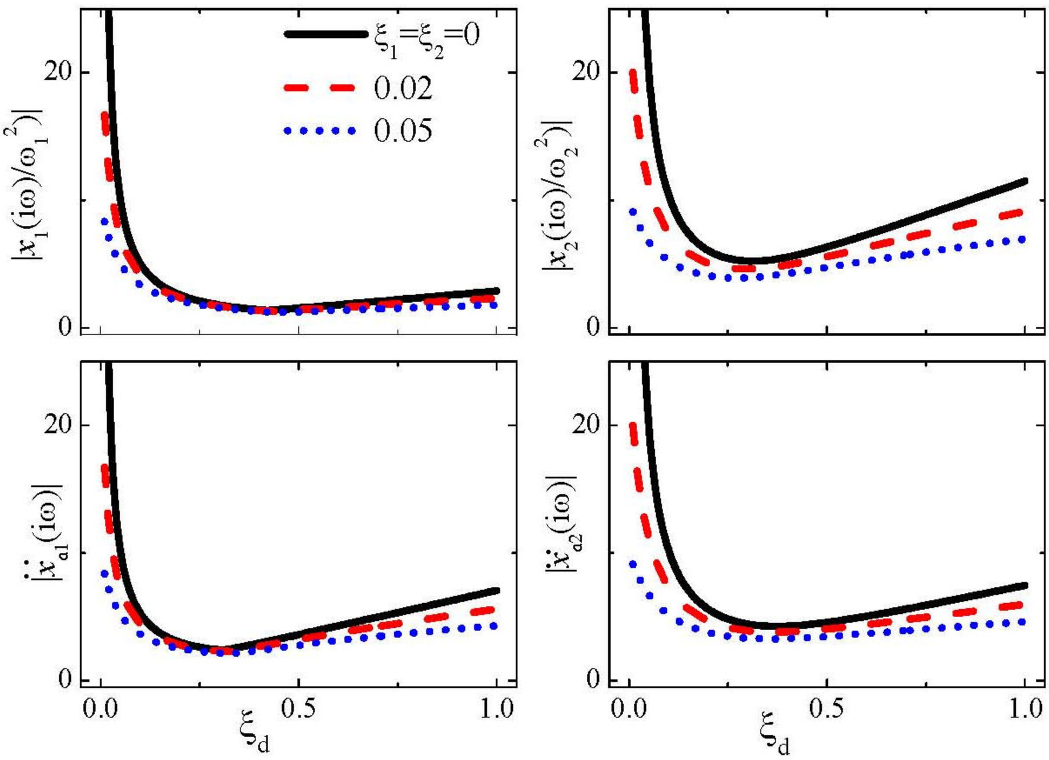

Fig. 6 Variation of response amplitude against the damping coefficient of the damper

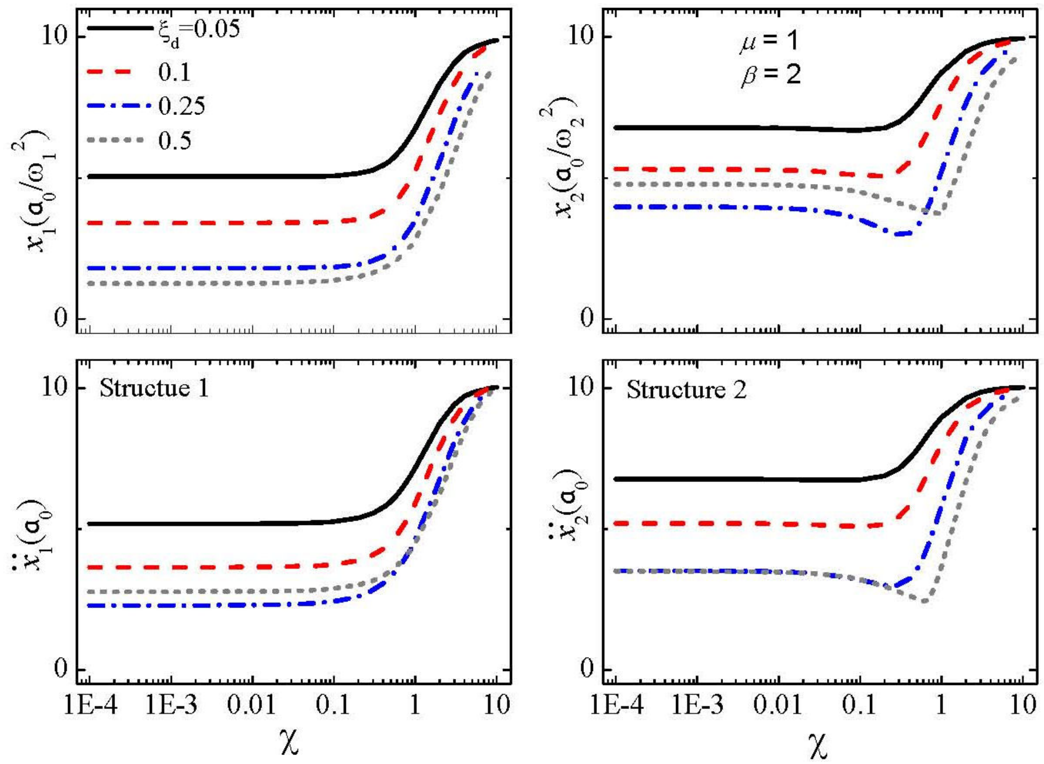

Fig. 7 Variation of peak response against relaxation time for the different value of the damping coefficient of the damper ($\beta = 2,\ \mu = 1$)

OPTIMUM DAMPER DAMPING FOR UNDAMPED CONNECTED STRUCTURES

The mean square displacement for an undamped system ($\Delta_1 = \Delta_2 = 0$) is obtained by solving Equations (15a) and (15b) for Structure 1 and 2, respectively, using the technique given in Cremer and Heckle [42] and are given by

$$\sigma_{x1}^2 = \pi S_0 \frac{(1+\mu)^3 \Delta_d^2 \omega_1^2 - 2\lambda\mu(1+\mu)\Delta_d \omega_1^2(\omega_1^2 - \omega_2^2) + \mu(1+\lambda^2\omega_1^2)(\omega_1^2 - \omega_2^2)^2}{\mu\Delta_d(\omega_1^3 - \omega_1\omega_2^2)^2} \tag{21a}$$

$$\sigma_{x2}^2 = \pi S_0 \frac{(1+\mu)^3 \Delta_d^2 \omega_2^2 + (\omega_1^2 - \omega_2^2)(\omega_1^2 + (-1 + 2\lambda(1+\mu)\Delta_d + \lambda^2\omega_1^2)\omega_2^2 - \lambda^2\omega_2^4)}{\mu\Delta_d(\omega_2^3 - \omega_2\omega_1^2)^2} \tag{21b}$$

The optimization criterion depends on the nature of dynamic load acting on the structure and response quantities of interest. Bhaskararao and Jangid [21] have considered the displacement and acceleration response of structures individually as response quantity for optimization. Zhu and Xu [19] have selected the relative vibration energy of the structure as the response quantity of interest for optimization. For the present study, the displacement and acceleration response of connected structure individually is considered for optimization. The optimizing condition $d\sigma_{x1}^2/d\xi_d = 0$ gives the optimum damping coefficient for a mean square displacement of Structure 1, after simplification, as

$$\xi_{d,\sigma_{x1}^2}^{opt} = \left| \frac{\left(\beta^2 - 1\right)\sqrt{\mu}\sqrt{1+\chi^2}}{2\left(1+\mu\right)^{3/2}} \right| \tag{22a}$$

Similarly for Structure 2, the optimum condition $d\sigma_{x2}^2/d\xi_d = 0$ results

$$\xi_{d,\sigma_{x2}^2}^{opt} = \left| \frac{\left(\beta^2 - 1\right)\sqrt{1+\beta^2\chi^2}}{2\beta\left(1+\mu\right)^{3/2}} \right| \tag{22b}$$

The corresponding mean square displacement of Structure 1 and 2 at the optimum damping of the damper obtained by using Equations (21) and (22) expressed as

$$\sigma_{x1,opt}^2 = \frac{2\pi\, S_0\left(1+\mu\right)\left(\sqrt{1+\mu} + \chi^2\sqrt{1+\mu} + \chi\sqrt{\mu}\sqrt{1+\chi^2}\right)}{\sqrt{\mu}\left(\beta^2-1\right)\sqrt{1+\chi^2}\,\omega_1^3} \tag{23a}$$

$$\sigma_{x2,opt}^2 = \frac{2\pi\, S_0\,\beta^2\left(1+\mu\right)\left(\sqrt{1+\mu} + \beta\chi\left(\beta\sqrt{1+\mu}\,\chi - \sqrt{1+\beta^2\chi^2}\right)\right)}{\left(\beta^2-1\right)\mu\sqrt{1+\beta^2\chi^2}\,\omega_2^3} \tag{23b}$$

To investigate the effect of frequency ratio of structures on the performance of Maxwell damper, the variation of ξ_d^{opt} and corresponding mean square displacement responses against the frequency ratio for the different mass ratio of structures and relaxation time χ = 0.01 is shown in Figure 7. From these figures, it is observed that the optimum damping coefficient increases with the increase of the frequency ratio. This is due to the reason that the higher frequency ratio increases the relative velocity between the connected floors and thus, requiring a higher damping coefficient. The Maxwell damper to be more effective for energy dissipation results in more reduction in displacement response. It is also observed that the increase in mass ratio reduces the ξ_d^{opt} of Maxwell damper. Further, with an increase in frequency ratio the mean square displacement of the connected structures is decreased. Thus, the Maxwell damper becomes more efficient for displacement response control of dynamically dissimilar coupled structures. The increases in mass ratio increase the mean square displacement response of Structure 1, whereas, it decreases the mean square displacement response of Structure 2.

In order to use the Equations (22) and (23), keep the Structure 1 as flexible among the two structure. When the Structure 2 is flexible in connected structures then the coupled system shall be rotated by 180 degree so that left side structure the Structure 1 become flexible and right side structure the Structure 2 as the stiff structure and calculate the system parameter accordingly so that frequency ratio, β shall always be achieved more than 1.

The mean square absolute acceleration for an undamped system ($\Delta_1 = \Delta_2 = 0$) is obtained by solving Equations (15c) and (15d) for Structure 1 and 2, respectively, using the technique given in Cremer and Heckle [42] and are given by

$$\sigma_{a1}^2 = \pi S_0 \frac{2\lambda\mu\Delta_d\omega_1^2\left(\omega_1^2-\omega_2^2\right)\left(\mu\omega_1^2+\omega_2^2\right) - \left(1+\mu\right)\Delta_d^2\left(\mu\omega_1^2+\omega_2^2\right)^2 - \mu\left(1+\lambda^2\omega_1^2\right)\left(\omega_1^3-\omega_1\omega_2^2\right)^2}{\mu\Delta_d\left(\omega_1^2-\omega_2^2\right)^2} \tag{24a}$$

$$\sigma_{a2}^2 = \pi S_0 \frac{2\lambda\Delta_d\omega_2^2\left(\omega_1^2-\omega_2^2\right)\left(\mu\omega_1^2+\omega_2^2\right) + \left(1+\mu\right)\Delta_d^2\left(\mu\omega_1^2+\omega_2^2\right)^2 + \left(1+\lambda^2\omega_2^2\right)\left(\omega_2^3-\omega_2\omega_1^2\right)^2}{\mu\Delta_d\left(\omega_1^2-\omega_2^2\right)^2} \tag{24b}$$

The optimizing condition $d\sigma_{a1}^2 / d\xi_d = 0$ gives the optimum damping coefficient for the mean square absolute acceleration of Structure 1, after simplification, as

$$\xi_{d,\sigma_{a1}^2}^{opt} = \left| \frac{\left(\beta^2-1\right)\sqrt{\mu}\sqrt{1+\chi^2}}{2\sqrt{1+\mu}\left(\beta^2+\mu\right)} \right| \tag{25a}$$

Similarly for Structure 2, the optimum condition $d\sigma_{a2}^2 / d\xi_d = 0$ results

$$\xi^{opt}_{d,\sigma^2_{a1}} = \left|\frac{\left(\beta^3-\beta\right)\sqrt{1+\beta^2\chi^2}}{2\sqrt{1+\mu}\left(\beta^2+\mu\right)}\right| \tag{25b}$$

The corresponding mean square acceleration of Structure 1 and 2 at the optimum damping of the damper obtained by using Equations (24) and (25) expressed as

$$\sigma^2_{a1,opt} = \frac{2\pi S_0\left(\beta^2+\mu\right)\left(\sqrt{1+\mu}+\chi^2\sqrt{1+\mu}+\chi\sqrt{\mu}\sqrt{1+\chi^2}\right)}{\sqrt{\mu}\left(\beta^2-1\right)\sqrt{1+\chi^2}}\omega_1 \tag{26a}$$

$$\sigma^2_{a2,opt} = \frac{2\pi S_0\left(\beta^2+\mu\right)\left(\sqrt{1+\mu}+\beta\chi\left(\beta\chi\sqrt{1+\mu}-\sqrt{1+\beta^2\chi^2}\right)\right)}{\left(\beta^2-1\right)\mu\sqrt{1+\beta^2\chi^2}}\omega_2 \tag{26b}$$

The effect of the frequency ratio of the connected structure on ξ^{opt}_d and corresponding mean square absolute acceleration response is shown in Figure 9 for the different mass ratio of structure and relaxation time $\chi = 0.01$. It is seen from these figures that the optimum damping coefficient ξ^{opt}_d increases with the increase of the frequency ratio as observed in Figure 8. Further increase in the mass ratio reduces the ξ^{opt}_d of Maxwell damper for acceleration responses. The increase in frequency ratio decreases the mean square absolute acceleration responses corresponding to respective ξ^{opt}_d of the two structures. Thus, it can be concluded that the higher reduction in the mean square acceleration responses can be achieved for dynamically dissimilar connected structures. The increase in mass ratio increases the mean square absolute acceleration response of Structure 1, whereas it decreases the mean square absolute acceleration response of Structure 2.

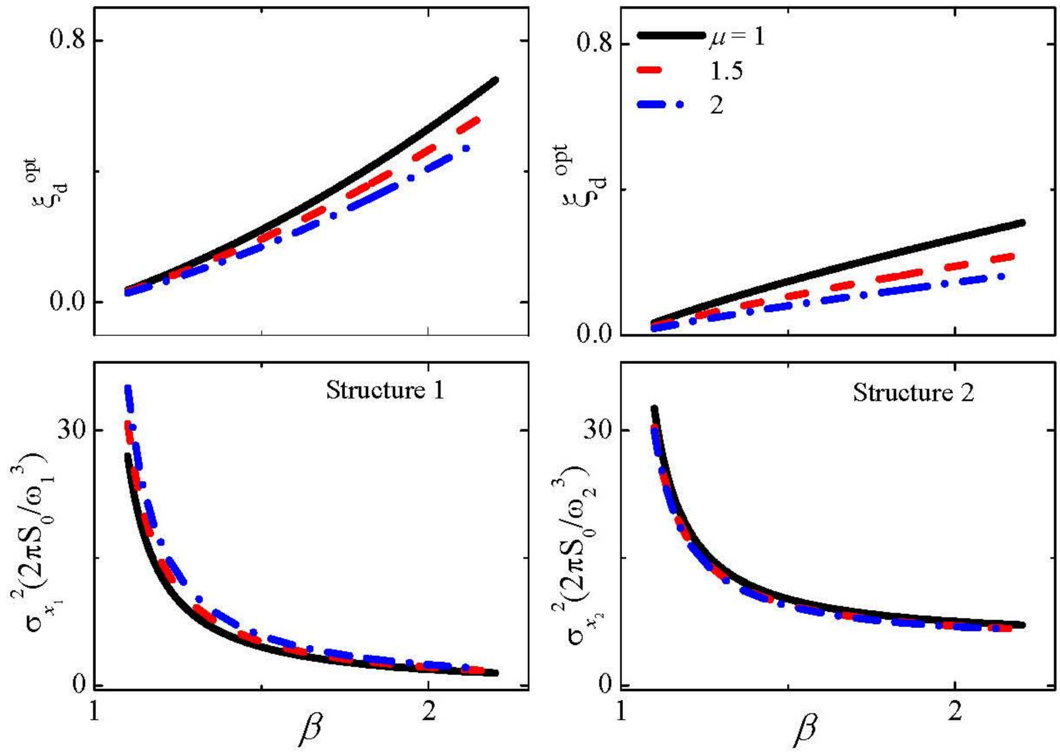

Fig. 8 Variation of the optimum damping coefficient of damper and corresponding mean square displacement responses against frequency ratio for different value of the mass ratio ($\chi = 0.01$)

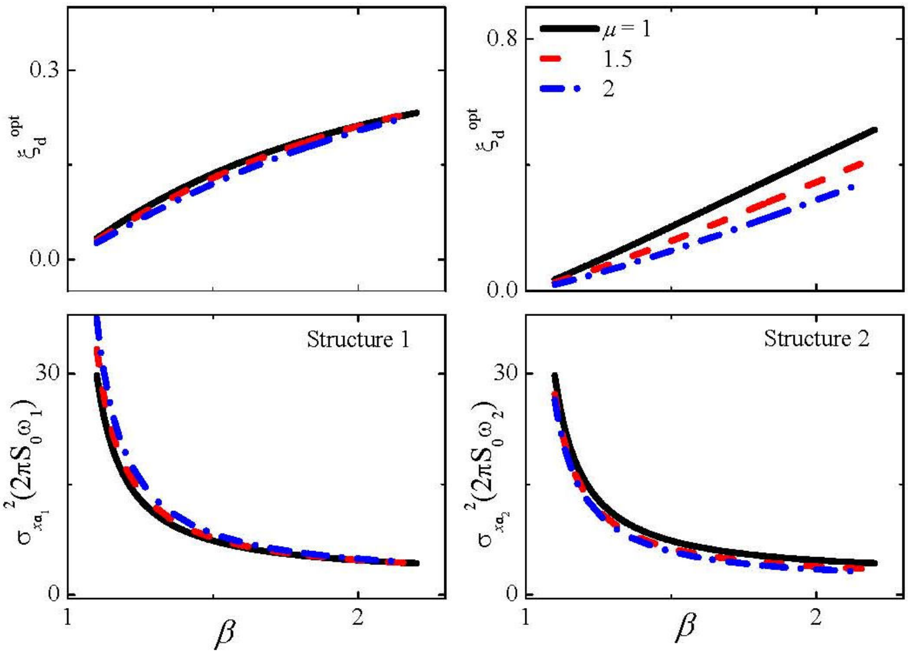

Fig. 9 Variation of the optimum damping coefficient of damper and corresponding mean square acceleration responses against frequency ratio for different value of the mass ratio ($\chi = 0.01$)

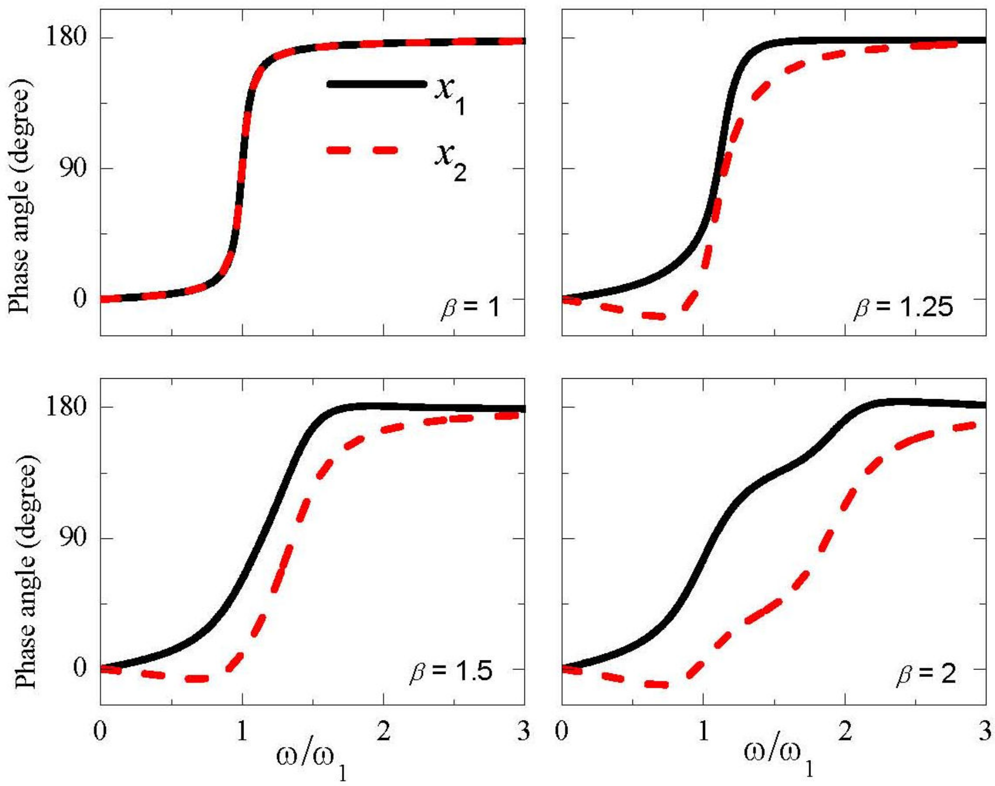

Fig. 10 Effects of frequency ratio on the phase angle of the displacement response of the connected structure ($\mu = 1$, $\xi_d = 0.21$ and $\chi = 0.01$)

To demonstrate the Maxwell damper performance for higher frequency ratio, the phase angle of the harmonic transfer function for displacement response of the Structure 1 and 2 considering $\mu = 1$,

ξ_d = 0.21 and $\chi = 0.01$ is plotted in Figure 10 for β = 1, 1.25, 1.5 and 2. The difference in the phase angle of the displacement of the two structures increases with an increase in the frequency ratio. This will result in larger relative displacement and velocity in Maxwell damper cause more energy dissipation and subsequent response reduction.

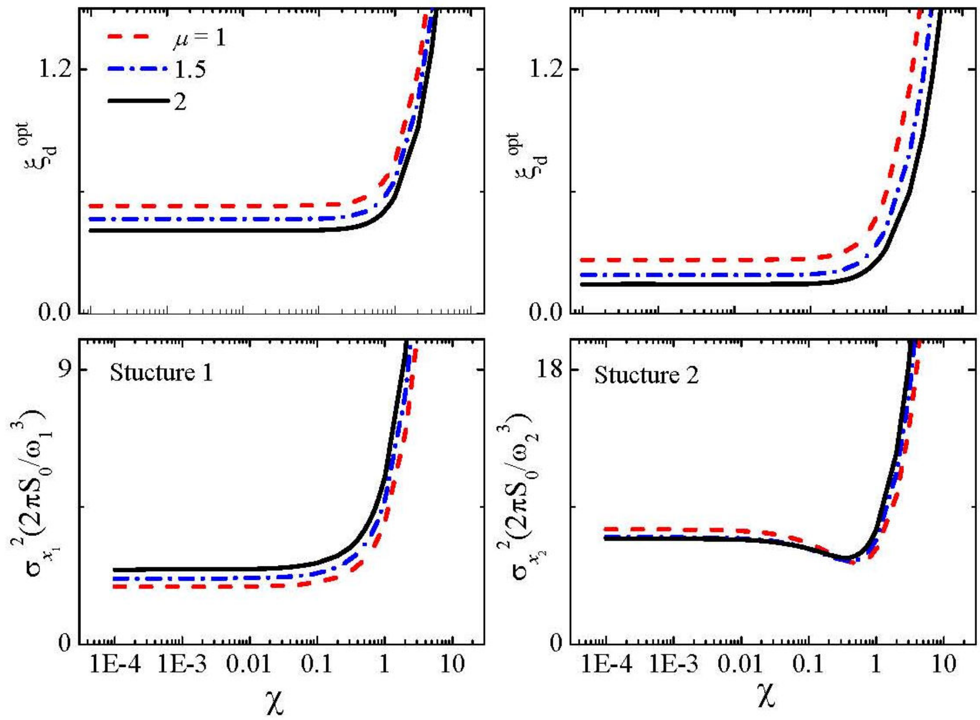

Fig. 11 Variation of the optimum damping coefficient of damper and corresponding mean square displacement response against relaxation time

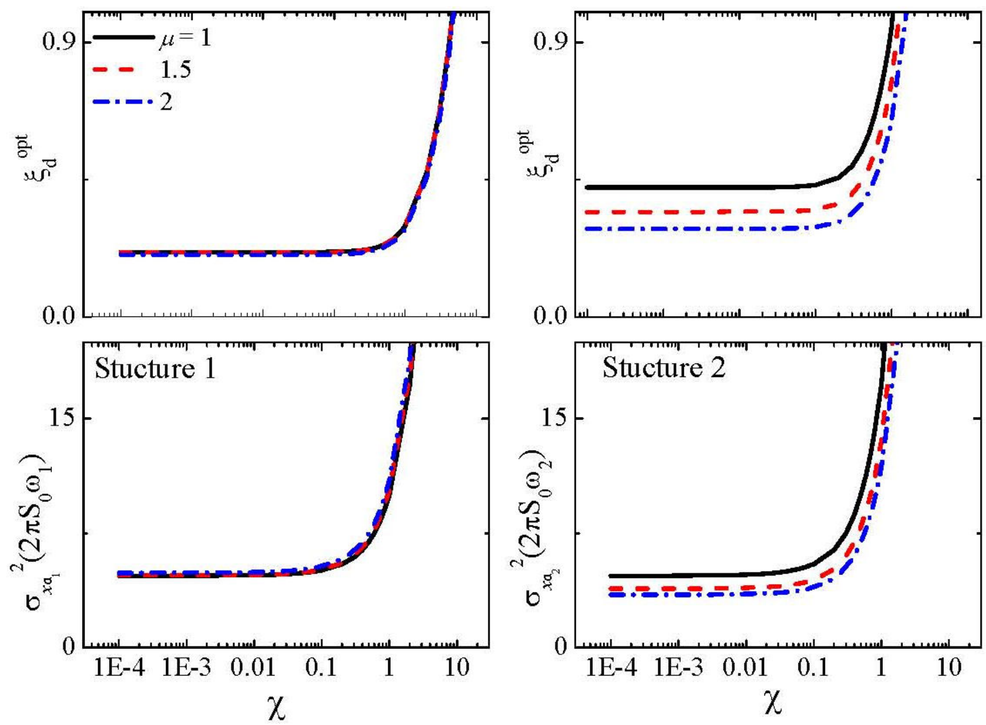

Fig. 12 Variation of the optimum damping coefficient of damper and corresponding mean square acceleration response against relaxation time

The effect of relaxation time χ on ξ_d^{opt} and the corresponding mean square displacement responses for mass ratio $\mu = 1$ and frequency ration $\beta = 2$ are shown in Figure 11. It is seen from these figures that increase in relaxation time χ up to the value of 0.1, the ξ_d^{opt} remain constant, further increase in χ, the ξ_d^{opt} increase. Thus, an increase in χ up to the value of 0.1 is not affecting the mean square displacement response of Structure 1. The increase in χ more than 0.1, the mean square displacement response of Structure 1 is increased. Whereas, increase in the χ up to the value of 0.01 is not affecting the optimum value of mean square displacement response of Structure 2, and further increase in the χ, the mean square displacement response of Structure 2 is decreased and after optimum value, increase in the χ, the mean square displacement response of Structure 2 is increased. Thus, the effect of relaxation time χ is marginal to the displacement response of Structure 1, whereas, the displacement response of Structure 2 (stiff structure) is sensitive to relaxation time χ. A similar effect is also observed in Figure 12, which shows the variation of optimum damping damper and corresponding acceleration response of Structure 1 and Structure 2, against relaxation time χ.

CONCLUSIONS

The random response of two parallel SDOF structures connected with Maxwell damper subjected to non-stationary as well as white-noise base excitation is investigated. Close-form expressions for optimum damping coefficient of Maxwell damper and corresponding mean square responses are derived. The effect of various parameters like frequency ratio, mass ratio, and relaxation time on the optimum damping coefficient of Maxwell damper and the corresponding mean square responses are is investigated. From the trends of the results of the present study, the following conclusions are drawn:

1. For a given parallel structure connected with Maxwell damper, there exists an optimum damping coefficient of the damper for which the displacement and absolute acceleration responses of connected structures attain the minimum value.
2. The optimum damping coefficient of the damper ξ_d^{opt} increases with the increase of the frequency ratio and decreases with the increase in the mass ratio. The corresponding response at optimum damper damping decreases with the increase in the frequency ratio.
3. The difference between the phase angle of response increase with the increase in frequency ratio results Maxwell damper is more effective for response control of the dynamically dissimilar connected structure.
4. Effect of relaxation time is very marginal on responses of flexible structure, whereas, the stiff structure is sensitive to the relaxation time of damper.
5. The derived close-form expressions for the optimum damping coefficient of the damper and corresponding responses can be effectively used for the preliminary optimum design of a parallel structural system connected with Maxwell damper.

REFERENCES

1. Housner, G.W., Bergman, L.A., Caughey, T.K., Ghassiakos, A.G., Claus, R.O., Mastri, S.F., Skelton, R.E., Soong, T.T., Spencer, B.F. and Yao, J.T.P. (1997). "Structural Control: Past, Present, and Future", *Journal of Engineering Mechanics, Vol. 123, No. 9, pp. 897-971.*
2. Soong, T.T. and Spencer, B.F. (2002). "Supplemental Energy Dissipation: State-of-the-Art and State-of-the-Practice", *Engineering Structures, Vol. 24, pp. 243-259.*
3. Dutta, T.K. (2003). "A State-of-the-Art Review on Active Control of Structure", *ISET Journal of Earthquake Technology, Vol. 40, No. 1, pp. 1-17.*
4. Kasai, K., Ooki, Y., Ishii, M., Ozaki, H., Ito, H., Motoyui, S., Hikino, T. and Sato, E. (2008). "Value-Added 5-Story Steel Frame and Its Components: Part-1 Full-Scale Damper Tests and Analysis", *The 14th World Conference on Earthquake Engineering, Beijing, China.*

5. Kasai, K., Nakai, M., Nakamura, Y., Asai, H., Suzuki, Y. and Ishii, M. (2008). "Current Status of Building Passive Control in Japan", *The 14th World Conference on Earthquake Engineering, Baijing, China.*
6. Kasai, K., Yaomin, Fu. and Atsushi, W. (1998). "Passive Control for Seismic Damage Mitigation", *Journal of Structural Engineering, ASCE, Vol. 124, No. 5, pp. 501-512.*
7. Soong, T.T. and Dargush, G.F. (1997). "Passive Energy Dissipation Systems in Structural Engineering", *Wiley, New York.*
8. Constantinou, M.C., Soong, T.T. and Dargush, G.F. (1998). "Passive Energy Dissipation System for Structural Design and Retrofit", *Monograph No. 1, Multidisciplinary Centre for Earthquake Engineering Research, Buffalo, N.Y.*
9. Constantinou, M.C. and Symans, M.D. (1993). "Seismic Response of Structures with Supplemental Damping", *Structural Design of Tall Buildings, Vol. 2, pp. 93-132.*
10. Makris, N. and Constantinou, M.C. (1991). "Fractional-Derivative Maxwell Model for Viscous Dampers", *Journal of Structural Engineering, ASCE, Vol. 117, No. 9, pp. 2708-2724.*
11. Singh, M.P., Verma, N.P. and Meroschi, L.M. (2003). "Seismic Analysis and Design with Maxwell Dampers", *Journal of Engineering Mechanics, ASCE, Vol. 129, No. 3, pp. 273-282.*
12. Lewandowski, R. and Chorazyczewski, B. (2010). "Identification of the Parameters of the Kelvin-Voigt and the Maxwell Fractional Models Used to Modeling of Viscoelastic Dampers", *Computers and Structures (Elsevier), Vol. 88, pp. 1-12.*
13. Greco, R. and Marano, G.C. (2015). "Identification of Parameters of Maxwell and Kelvin-Viogt Generalized Models for Fluid Viscous Dampers", *Journal of Vibration and Control, Vol. 21, No. 2, pp. 260-274.*
14. Xiao, R., Sun, H. and Chen, W. (2016). "An Equivalence Between Generalized Maxwell Model and Fractional Zener Model", *Mechanics of Materials, Elsevier, Vol. 100, pp. 148-153.*
15. Kasai, K. and Maison, B.F. (1992). "Dynamics of Pounding when Two Buildings Collide", *Earthquake Engineering and Structural Dynamics, Vol. 21, pp. 771-786.*
16. Jeng, V. and Kasai, K. (1996). "Spectral Relative Motion of Two Structures Due to Seismic Travel Waves", *Journal of Structural Engineering, ASCE, Vol. 122, No. 10, pp. 1128-1135.*
17. Zhang ,W.S. and Xu, Y.L. (2000). "Vibration Analysis of Two Buildings Linked by Maxwell Model-Defined Fluid Dampers", *Journal of Sound and Vibration, Vol. 233, No. 5, pp. 775-796.*
18. Yang, Z., Xu, Y.L. and Lu, X.L. (2003). "Experimental Seismic Study of Adjacent Buildings with Fluid Dampers", *Journal of Structural Engineering, ASCE, Vol. 129, No. 2, pp. 197-205.*
19. Zhu, H.P. and Xu, Y.L. (2005). "Optimum Parameters of Maxwell Model-Defined Dampers Used to Link Adjacent Structures", *Journal of Sound and Vibration, Elsevier, Vol. 279, pp. 253-274.*
20. Matsagar, V.A. and Jangid, R.S. (2005). "Viscoelastic Damper Connected to Adjacent Structures Involving Seismic Isolation", *Journal of Civil Engineering and Management, Vol. 11, No. 4, pp. 309-322.*
21. Bhaskararao, A.V. and Jangid, R.S. (2007). "Optimum Viscous Damper for Connecting Adjacent SDOF Structures for Harmonic and Stationary White-Noise Random Excitations", *Earthquake Engineering and Structural Dynamics, Vol. 36, pp. 563-571.*
22. Patel, C.C. and Jangid, R.S. (2010). "Seismic Response of Adjacent Structures Connected with Maxwell Dampers", *Asian Journal of Civil Engineering (Building and Housing), Vol. 11, No. 5, pp. 585-603.*
23. Zhu, H.P., Ge, D.D. and Huang, X. (2011). "Optimum Connecting Dampers to Reduce the Seismic Responses of Parallel Structures", *Journal of Sound and Vibration, Vol. 330, pp. 1931-1949*.
24. Reza, Milanchian, Mahmood, Hosseini and Masoud, Nekooei (2017). "Vertical Isolation of a Structure Based on Different States of Seismic Performance", *Earthquake and Structure, Vol. 13, pp. 103-118.*
25. Bird, R.B., Armstrong, R.C. and Hassager, O. (1987). "Dynamics of Polymeric Liquids", *Wiley, New York.*

26. Housner, G.W. (1955). "Properties of Strong Ground Motion Earthquakes", *Bulletin of Seismological Society of America, Vol. 45, pp. 197-218*.
27. Thomson, W.T. (1959). "Spectral Aspect of Earthquakes", *Bulletin of Seismological Society of America, Vol. 49, pp. 91-98*.
28. Rosenblueth, F. and Bustamante, J. (1962). "Duration of Structural Response to Earthquakes", *Journal of Engineering Mechanics Division, ASCE, EM3, Vol. 88, pp. 75-106*.
29. Kanai, K. (1957). "Semi-Imperical Formula for the Seismic Characteristics of the Ground", *Univ. Tokyo Bull., Earthquake Res. Inst., Tokyo, Japan, Vol. 35, pp. 309-325*.
30. Tajimi, H. (1960). "A Statistical Method of Determining the Maximum Response of a Building Structure During an Earthquake", *Proceeding of 2nd World Conference on Earthquake Engineering, Vol. 2, pp. 781-798*.
31. Shinozuka, M. and Sato, Y. (1967). "Simulation of Non-Stationary Random Process", *Journal of Engineering Mechanics, ASCE, Vol. 93, pp. 11-40*.
32. Iyengar, R.N. and Iyengar, K.T.S. (1969). "A Non-Stationary Random Process Model for Earthquake Acceleration", *Bulletin of the Seismological Society of America, Vol. 59, pp. 1163-1188*.
33. Amin, M. and Ang, A.H.S. (1968). "Non-Stationary Stochastic Model of Earthquake Motion", *Journal of Engineering Mechanics, ASCE, Vol. 94, pp. 559-583*.
34. Clough, R.W. and Penzien, J. (1993). "Dynamics of Structures", *McGraw-Hill, New York*.
35. Jangid, R.S. (2004). "Response of SDOF System to Non-Stationary Earthquake Excitation", *Earthquake Engineering and Structural Dynamics, Vol. 33, pp. 1417-1428*.
36. Gasparini, D.A. (1979). "A Response of MDOF System to Non-Stationary Random Excitation", *Journal of Engineering Mechanics Division, ASCE, Vol. 105 (EM1), pp. 13-27*.
37. Langley, R.S. (1986). "Structural Response to Non-Stationary Non-White Stochastic Ground Motion", *Earthquake Engineering and Structural Dynamics, Vol. 14, pp. 909-924*.
38. Muscolino, G. (1988). "Non-Stationary Envelop in Random Vibration Theory", *Journal of Engineering Mechanics Division, ASCE, Vol. 114, No. 8, pp. 1396-1413*.
39. Hammond, J.K. (1968). "On the Response of Single and Multi-Degree of Freedom System to Non-Stationary Random Excitation", *Journal of Sound and Vibration, Vol. 7, No. 3, pp. 393-416*.
40. Corotis, R.B. and Vanmarcke, E.H. (1975). "Time Dependent Spectral Content of System Response", *Journal of Engineering Mechanics Division, ASCE, Vol. 101 (EMS), pp. 623-637.*
41. Nigam, N.C. (1983). "Introduction to Random Vibration", *MIT Press, Cambridge*.
42. Cremer, L. and Heckl, M. (1973). "Structure Borne Sound", *Springer Verlag, New York*.